Shape and Symmetry of Heptacoordinate Transition-Metal Complexes: Structural Trends

David Casanova,[a] Pere Alemany,*[b] Josep M. Bofill,[c] and Santiago Alvarez*[a]

Abstract: The stereochemistries of heptacoordinate transition-metal complexes are analyzed by using continuous symmetry and shape measures of their coordination spheres. The distribution of heptacoordination through the transition-metal series is presented based on structural database searches including organometallic and Werner-type molecular complexes, metalloproteins, and extended solids. The most common polyhedron seems to be the pentagonal bipyramid, while different preferences are found for specific families of compounds, as in the complexes with three or four carbonyl or phosphine ligands, which prefer the capped octahedron or the capped trigonal prism rather than the pentagonal bipyramid. The symmetry maps for heptacoordination are presented and shown to be helpful for detecting stereochemical trends. The maximal symmetry interconversion pathways between the three most common polyhedra are defined in terms of symmetry constants and a large number of experimental structures are seen to fall along those paths.

Keywords: continuous symmetry measures · coordination modes · metal complexes · structure correlations · symmetry maps

Introduction

Interest in heptacoordination has experienced a resurgence in recent years, from the preparation of ferromagnetic compounds using heptacyanometalate building blocks,[1] to structures of new homoleptic heptacoordinate complexes[2, 3] such as $[MoMe_7]^-$ or $[ReF_7]$ and the use of halocarbonyl seven-coordinate Mo and W complexes as versatile starting materials in a number of synthetic reactions.[4] Furthermore, heptacoordinate complexes are interesting as intermediates in associative reactions of six-coordinate complexes and in dissociative reactions of eight-coordinate ones.[5] Finally, a few active centers in metalloproteins seem to be heptacoordinate, such as the Mo center in the oxidized form of a dmso reductase,[6, 7] manganese atoms in glutamine synthetase,[8] inositol monophosphatase[9] complexed by troponin (a calcium-binding protein)[10] or in L-fucose isomerase from *Escherichia Coli*,[11] and Cd centers in the cytochrome domain of cellobiose oxidase[12] or complexed by hydrolases.[10, 13, 14] Several reviews on heptacoordination have been published, although extensive data compilation and detailed discussions date back to 1985.[4, 15–18]

The relative abundance of heptacoordinate complexes is generally a matter that is dealt with in a rather subjective way. Hence, in most textbooks or treatises on stereochemistry it is under-represented: only a few examples are given, which say little about the variety of chemical species nowadays known. A completely opposite view is given in a review devoted to heptacoordinated molybdenum compounds: "*coordination number seven dominates much of the coordination chemistry of molybdenum*".[17] A simple structural database search tells us that neither of the two extreme views gives an adequate account of the abundance of heptacoordinated transition metal complexes. It is therefore convenient to make a brief survey of the abundance and distribution of heptacoordination in transition-metal chemistry, based on a structural database analysis. Coordination number seven is not common in transition-metal chemistry: an estimate based on the number of transition-metal σ-bonded complexes found in the Cambridge Structural Database reveals that heptacoordi-

[a] Prof. S. Alvarez, M. Sc. D. Casanova
Departament de Química Inorgànica and
Centre de Recerca en Química Teòrica (CeRQT)
Universitat de Barcelona
Diagonal 647, 08028 Barcelona (Spain)
Fax: (+34) 93-490-7725
E-mail: santiago@qi.ub.es

[b] Dr P. Alemany
Departament de Química Física and
Centre de Recerca en Química Teòrica (CeRQT)
Universitat de Barcelona
Diagonal 647, 08028 Barcelona (Spain)

[c] Dr J. M. Bofill
Departament de Química Orgànica and
Centre de Recerca en Química Teòrica (CeRQT)
Universitat de Barcelona
Diagonal 647, 08028 Barcelona (Spain)

Supporting information for this article is available on the WWW under http://www.chemeurj.org or from the author: tables of refcodes, relevant structural information, and calculated symmetry measures.

  0947-6539/03/0906-1281 $ 20.00+.50/0

nate complexes represent 1.8% of the total number of structures reported (see Database Searches section). The distribution of heptacoordination throughout the transition metal series is also peculiar (Figure 1): for late transition metals (Groups 7–11), heptacoordination seems to be more

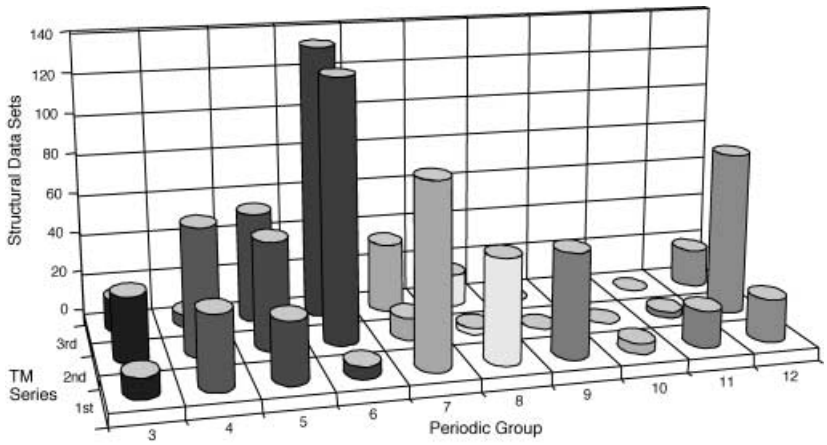

Figure 1. Distribution of σ-heptacoordinate complexes through the transition metal series.

common for the first-row metal than for its heavier congeners, whereas for early (Groups 3–6) and Zn Group metals heptacoordination is more common for second- or third-row elements. On the other hand, heptacoordination is, in general, less common for the late than for the early transition metals, with no structures found for Rh, Ir, Pd, Pt, or Au. Unlike the late transition metals, the Zn group metals again present quite a large number of examples of heptacoordination. An intriguing anomaly is found for Cr, for which few heptacoordinate complexes are found, in contrast with its first-row neighbors and with the heavier elements of the same group.

Seven being an odd coordination number, no regular polyhedron can describe the coordination sphere around a heptacoordinated metal atom. The most commonly used polyhedra have two (the pentagonal bipyramid (PBP), **1**) or three (the capped octahedron (CO) **2** and the capped trigonal prism (CTP) **3**) types of vertices in different proportions, which should allow for easy identification of the stereochemistry through NMR spectroscopy in solution or by infrared spectroscopy in the solid state.[19] However, very often one observes solution spectra consistent with seven equivalent ligands due to the existence of low-barrier fluxional processes.[5, 20] Single crystal X-ray crystallography seems to be better adapted to fully characterize the stereochemistry of a given heptacoordinate molecule, yet it is not easy to decide by visual inspection or by a simple analysis of the bond angles on the most appropriate coordination polyhedron. This is especially because in many instances the site symmetry in the crystal is lower than the D_{5h}, C_{3v}, and C_{2v} symmetries of the ideal polyhedra **1**–**3**. In addition to the three polyhedra already mentioned (**1**–**3**), we will also take into account other less likely arrangements, such as the hexagonal pyramid (**4**), the heptagon (**5**), or the so called 4:3 geometry (**6**). For simplicity we will refer to these polyhedra with the commonly employed acronyms reflected in **1**–**6**.

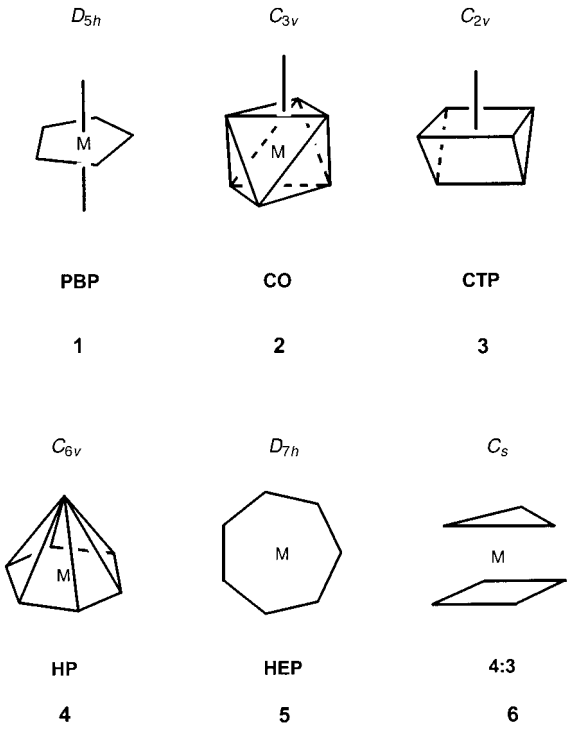

It had been suggested[21, 22] that crystal structure data offer a guide to reaction pathways between polytopes, specifically in that distortions from ideal geometry follow explicit geometric reaction paths, and this has been well demonstrated for

Abstract in Catalan: *Les estereoquímiques dels complexos de metalls de transició heptacoordinats han estat analitzades emprant les mesures contínues de simetria i de forma de llurs esferes de coordinació. Es presenta la distribució de l'heptacoordinació al llarg de les sèries de metalls de transició, d'acord amb els resultats de cerques de bases de dades estructurals que inclouen complexos moleculars organometàllics i de tipus Werner, així com metal·loproteïnes i sòlids estesos. El políedre més comú sembla ser la bipiràmide pentagonal, mentre que per famílies concretes de compostos es troben diferents preferències, com en el cas dels complexos amb tres o quatre lligands carbonil o fosfina, que prefereixen l'octaedre cofiat o el prisma trigonal cofiat. Es presenten els mapes de simetria per a l'heptacoordinació i es mostra que aquests poden ser d'utilitat per detectar tendències estereoquímiques. Els camins de màxima simetria per a la interconversió dels tres políedres més comuns es defineixen en funció d'unes constants de simetria i es troba que un gran nombre d'estructures experimentals es situen al llarg d'aquests camins.*

  0947-6539/03/0906-1282 $ 20.00+.50/0 *Chem. Eur. J.* **2003**, *9*, No. 6

pentacoordinate complexes.[23] A theoretical analysis of the stereochemistry of heptacoordinate complexes based on a point charge model has been presented by Kepert.[24] He found, however, that differences between the three characteristic polyhedra are rather small, both in energy and in geometry, since only small angular displacements of the ligands can take one from one polyhedron to the other. A molecular orbital analysis of bonding and stereochemistry in heptacoordinate complexes was reported by Hoffmann and co-workers,[22] based on extended Hückel calculations. More recently, Lin and Bytheway[25] performed ab initio Hartree–Fock calculations on d^0-fluoro complexes $[MoF_7]^-$, $[WF_7]^-$, and $[ReOF_6]^-$, and concluded that the CO and CTP structures have approximately the same energy for the heptafluoro complexes and are more stable than the pentagonal bipyramidal geometry by approximately $1-4\ kcal\,mol^{-1}$. In contrast, for $[ReOF_6]^-$ the PB geometry was calculated to be more stable than CO and CTP by some $28\ kcal\,mol^{-1}$. However, the same authors note that experimental structures of heptafluoro complexes can be found in any of the three polyhedra.

The continuous symmetry (or shape) measures (CSM) proposed by Avnir and coworkers[26, 27] essentially allow one to numerically evaluate by how much a particular structure deviates from an ideal symmetry or from an ideal shape (such as a polyhedron). The continuous shape measure relative to a polyhedron A for a set of N atoms (in the present case the set of atoms analyzed comprises the metal and the seven donor atoms, thus $N=8$), characterized by their position vectors Q_i, is defined according to Equation (1), where P_i is the position vector of the corresponding vertex in the reference polyhedron A and Q_0 is the position vector of the geometrical center of the problem structure.

$$S(A) = \min \frac{\sum_{I=1}^{N} |Q_i - P_i|^2}{\sum_{I=1}^{N} |Q_i - Q_0|^2} \cdot 100 \qquad (1)$$

The minimum is taken for all possible relative orientations in space, scale factor, and for all possible mappings of the vertices of the problem and the reference polyhedra. For the study of coordination compounds, only those vertex permutations that leave the metal atom in the center of the polyhedron are considered. With such a definition, $S(A)=0$ corresponds to a structure fully coincident in shape with the reference polyhedron and the maximum allowed value of $S(A)$ is 100, which corresponds to the hypothetical case in which all eight atoms occupy the same position in space.

For those cases in which the choice of a reference polyhedron with a given symmetry is not unique we have actually two alternative choices for the definition of its P_i coordinates: either we search for the nearest polyhedron that has the desired symmetry or we establish a conventional polyhedron relative to which we will calculate the measures using Equation (1). The symmetry criterion is in general less restrictive than the definition of a conventional polyhedron, so we term the two approaches *continuous symmetry measures* and *continuous shape measures*, respectively. As an example, consider the trigonal pyramids shown in **7**. All of them have

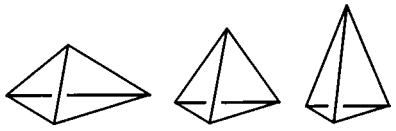

7

the full C_{3v} symmetry, and consequently have symmetry measures $S(C_{3v})=0$. If we were to consider the central figure as a conventional trigonal pyramid (cTP), we would obtain nonzero shape measures S(cTP) for the other two pyramids. For practical purposes, we find it more adequate in the case of seven-vertex polyhedra to define conventional reference polyhedra, and the corresponding shape measures will be used throughout this paper. Complementarily, we will also use symmetry measures to identify the presence of a given symmetry element, such as the fivefold rotation axis in the pentagonal bipyramid.

Drew reported a least-squares procedure to assign the stereochemistry of heptacoordinate complexes,[15] and a similar approach has been more recently proposed by Maseras and Eisenstein,[28] but the assignment of a coordination polyhedron is still in most cases done in a non systematic way. A related approach applied by Allen and coworkers to the study of the shape of heptacoordinate complexes consists in analyzing the $n(n-1)/2$ bond angles of an ML_n core and use of a Euclidean dissimilarity metric as a one-dimensional comparator of those angles.[29, 30] Compared to the least-squares algorithm proposed by Drew and by Maseras and Eisenstein, the CSM formalism has the advantage that the resulting measures are size-normalized and allows one to compare on the same scale the deviation from a particular polyhedron of a diversity of molecules, or the deviation of a particular molecule from different polyhedra. Compared to the dissimilarity measures proposed by Allen and co-workers, the CSM approach has the advantage that it takes into account not only angular but also distance distortions. Previous work in our group has investigated what we can learn from continuous symmetry measures about the structural trends of transition metal compounds with coordination numbers four,[31] five,[32] or six.[33] The objective of the present work is to establish the general criteria for the continuous symmetry analysis of the seven-vertex polyhedra and to investigate whether the use of such an approach can offer us some new insight into the general structural trends of heptacoordinate transition-metal compounds.

Database searches: From the Cambridge Structural Database[34] (version 5.23), compounds with a metal atom defined in the database as heptacoordinate and belonging to any of the periodic Groups 3 through 12 were retrieved with the following restrictions: no π-bonded ligands were allowed, no direct bonds between donor atoms coordinated to the metal were allowed, and structures with agreement factors R larger than 10% as well as disordered structures were disregarded. As donor atoms we considered any element of Groups 14–17 or hydrogen. A total of 791 compounds were found, comprising 968 crystallographically independent structural data sets. Removal of the restraint of heptacoordination resulted in a total of 43319 structures retrieved, indicating a relative

abundance of heptacoordination of 1.8%. For inorganic compounds, searches were carried out in the Karlsruhe database (ICSD, version 2001/2) for binary or ternary compounds with isolated MX_7 units (X = F, O, CO, or CN), and a total of 24 structural data sets were found. Heptacoordinate transition-metal sites in metallobiomolecules were retrieved with the help of the Metalloprotein Database (MDB, 13 structures found).[35]

Conventional Seven Vertices Polyhedra and Symmetry Maps

Of the seven-vertex shapes considered, only the heptagon is fully determined by symmetry and its shape and symmetry measures are thus equivalent. In all other cases, an infinite number of polyhedra exist with the given symmetry, shape therefore being a more stringent criterion than symmetry, and for practical purposes we find it more adequate to define a unique reference shape for each symmetric set of ideal polyhedra. Let us consider as an example the capped octahedron, which has ideal C_{3v} symmetry. There is a wide structural variability within the C_{3v} symmetry, since there are three independent sets of bond lengths and two independent sets of bond angles (a, b, c, α, and β in **8**), and it seems

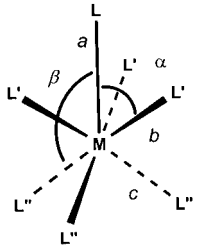

8

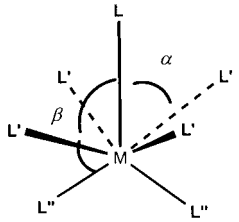

9

therefore more adequate to choose one specific capped octahedron as a reference shape with which to compare the experimental structural data. On one hand, we had previously observed that small differences in metal–ligand bond lengths do not significantly affect the symmetry measures and a criterion for ideality applied for other coordination numbers consists of requiring all distances from the vertices to the center of the polyhedron to be the same, $a = b = c$, that is, the radius of the *coordination sphere* around the central atom or ion.[32] In addition, we observe that α bond angles (72–77°) in homoleptic complexes are systematically larger than the corresponding values in the octahedron (54.7°), whereas the β angles (117–137°) can be smaller or larger than in the octahedron (125.3°), while the minimum interligand repulsion is found at $73.3 \le \alpha \le 75.8°$ and $128.8 \le \beta \le 131.4°$ according to point charges calculations,[36] or $70 \le \alpha \le 84°$ and $127 \le \beta \le 138°$ from molecular orbital calculations.[22] Considering all these data, the criterion of ideality for the CO adopted by Drew ($\alpha = 74.1°, \beta = 125.5°$)[15] seems a reasonable one. Those values were found in the structure of the $[W(CO)_4Br_3]^-$ ion,[37] which has crystallographically imposed C_{3v} symmetry. From here on we will refer to that structure as the *conventional capped octahedron* and refer to all the corresponding shape measures as S(cCO). It is important to keep in mind the possibility of a given molecule having a perfectly C_{3v} capped octahedron symmetry but with different geometrical parameters than in our conventional CO, resulting in nonzero S(cCO) values. The uncertainty in the S(cCO) values can be dealt with in two ways: 1) by considering as significant only differences in shape measures that are beyond the uncertainty due to the choice of the reference polyhedron, and 2) by checking the existence of a C_3 symmetry axis with the corresponding $S(C_3)$ symmetry measures.

In Figure 2a we show how S(cCO) varies for C_{3v} heptahedra with varying α or β angles (see **8**). There it can be seen that for angle variations of $\pm 5°$, S(cCO) adpots values of 0.2 at most. Hence, for the time being we take 0.1 as the typical uncertainty in our symmetry measures due to the adoption of a conventional capped octahedron among the infinite number of possible C_{3v} heptahedra, but the calculated values will be given with two decimal figures for internal consistency. We will come back to this issue after analyzing experimental structures to apply the second criterion, that is, comparison with $S(C_3)$ values.

Similarly, our definition of a conventional CTP (**9**) corresponds to seven identical metal–ligand distances, a square geometry for the capped face and bond angles $\alpha = 82°$ and $\beta = 144.25°$, also adequately providing a representative geometry of point charges,[36] molecular orbital,[22] and experimental data analyzed by us below. As found for the CO, the uncertainty associated with the choice of a conventional polyhedron (Figure 2b) can be evaluated as approximately 0.2. Finally, for the PBP the only convention we adopt is that the seven bond distances are identical, since the rest of the bonding parameters are determined by the D_{5h} symmetry, and the uncertainty relative to a $S(D_{5h})$ measure is estimated to be about 0.01. For the hexagonal pyramid, our reference polyhedron is one with seven identical metal–ligand distances and with the metal atom in the center of the basal hexagon.

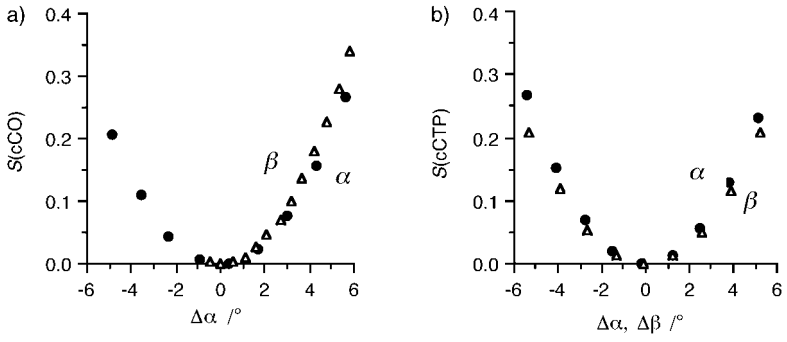

Figure 2. Variation of the S(cCO) and S(cCTP) values as a function of the deviation of angles α (circles) and β (triangles) described in **8** and **9** from the values adopted in our conventional reference polyhedra.

0947-6539/03/0906-1284 $ 20.00+.50/0 *Chem. Eur. J.* **2003**, *9*, No. 6

If fortunate when analyzing a given molecular structure, we can find a conventional polyhedron that describes to a good approximation the experimental coordination sphere, that is, S(polyhedron) < 1.0, which our experience with other coordination numbers indicates represents minor deviations from ideality. In most cases, however, significant deviations from ideality are found for all the relevant polyhedra. We can, of course, compare the different values—S(cCO), S(cCTP), and S(PBP) in the present case—and take the smallest one to describe the coordination polyhedron. However, such a mode of operation does not guarantee that a sensible description of the molecular structure is obtained, since some cases may be found in which the geometry cannot be appropriately described by any of the polyhedra chosen. For that purpose it seems more appropriate to use symmetry maps that have been explored for other coordination numbers by us recently.[31, 33] A symmetry map is just a scatterplot of the symmetry measures corresponding to two different polyhedra with the same number of vertices. In the case of heptacoordination, we will systematically use two symmetry maps in which we represent either S(cCTP) or S(PBP) as a function of S(cCO).

The calculated values of the shape measures for the reference structures **1**–**6** are given in Table 1 and plotted in the CO-CTP symmetry map (Figure 3). By definition, the cCO has S(cCO) = 0, and it is found that its corresponding deviation from the cCTP is 1.53, which is rather small compared to those between, for example, the octahedron and the trigonal prism, 16.74,[33] or between the tetrahedron and the square, 33.33.[31] At the other extreme, the heptagon is seen to be far away from the rest of the ideal heptahedra. It can also be seen that the separation between two polyhedra depends essentially on their bi- or tridimensional character. Thus, the nearly spherical cCO and cCTP are close to each other (1.53), the ellipsoidal PBP is somewhat farther from the two nearly-spherical structures (6.6–8.4), the hemispherical HP is still farther (17–20), and the two-dimensional heptagon is at a still larger separation (35–38). This is best seen in the symmetry map (Figure 3a), where we represent S(cCTP) as a function of S(cCO). Further reduction of dimensionality leads to systems that are unattainable in a coordination compound, but a geometry in which the seven ligands have collapsed at the central atom has the largest possible values of both S(cCO) and S(cCTP), 100.

Table 1. Shape measures of seven-vertex polyhedra (**1**–**6**) relative to each other.

	PBP	cCO	cCTP	HP	HEP
PBP	0.000	8.404	6.641	26.688	35.213
cCO		0.000	1.528	17.056	37.774
cCTP			0.000	19.951	35.874
HP				0.000	25.468

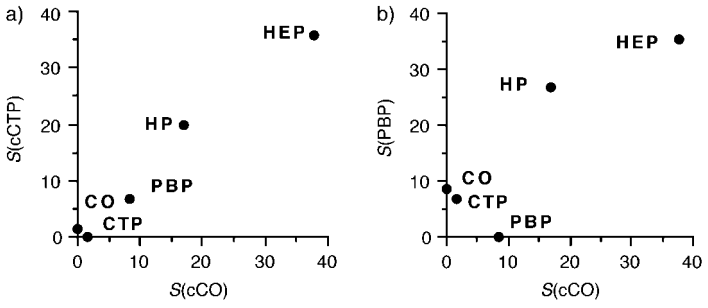

Figure 3. Position of the heptahedra **1**–**6** in the cCO-cCTP (a) and cCO-PBP (b) symmetry maps.

An alternative symmetry map that will be used below is obtained by representing S(PBP) as a function of S(cCO), illustrated in Figure 3b for the conventional polyhedra. Again, the proximity of cCO and cCTP and the increasing difference with increasing separation in dimensionality are easily recognized in such a representation.

An additional seven-vertex polyhedron that we have considered is a trigonal prism with a capped trigonal face. The position of a variety of such capped trigonal prisms in the two symmetry maps considered is close to that of the hexagonal pyramid (HP in Figure 3). There are a wealth of possible trigonal face-capped trigonal prisms with C_{3v} symmetry, similar to what has been discussed for the CO, and the average values of their shape measures, together with their deviations, are as follows: S(PBP) = 23.2 (1.2), S(cCO) = 17.8 (1.4) and S(cCTP) = 18.3 (1.0).

Which polyhedron?: In this section we ask ourselves: Are the experimental structures reasonably described by the conventional polyhedra? Which is the preferred polyhedron among heptacoordinate compounds? Are any of the available polyhedra favored by a certain metal or electron configuration or by a specific type of ligand? Before trying to address such questions, let us show by way of a few examples how the use of the continuous symmetry measures provides a sensible criterion to assign the coordination polyhedron, a task which is otherwise not easy. First, we show in Figure 4 the molecular structures of three heptacoordinate compounds, outlining the edges of alternative polyhedra to stress how a visual inspection leads to the conclusion that the same structure resembles more than one reference polyhedron. We leave it to the reader to identify which is the best description according to the CSM criterion with the help of the values given later (see Table 6). A second case is provided by halo-carbonyl tungsten complexes given by Baker[4] as examples of the ideal polyhedra. The symmetry measures (Table 2) clearly indicate that assignment of an ideal polyhedron is not always granted and in the case of $[WI(acac)(CO)_2(PEt_3)_2]$ the proposed pentagonal bipyramid is not a better choice than the CO or the CTP.

To answer the above questions we have analyzed the structures of a variety of heptacoordinate transition-metal compounds from structural databases, as indicated in the Database Searches section. For all the selected structures we have calculated their shape measures relative to PBP, cCO, and cCTP (**1**–**3**) and assigned to each structure the closest ideal polyhedron. First we do this for the whole set of heptacoordinate σ-bonded complexes and then we will analyze some representative families individually. In a subsequent section we will consider how accurate those

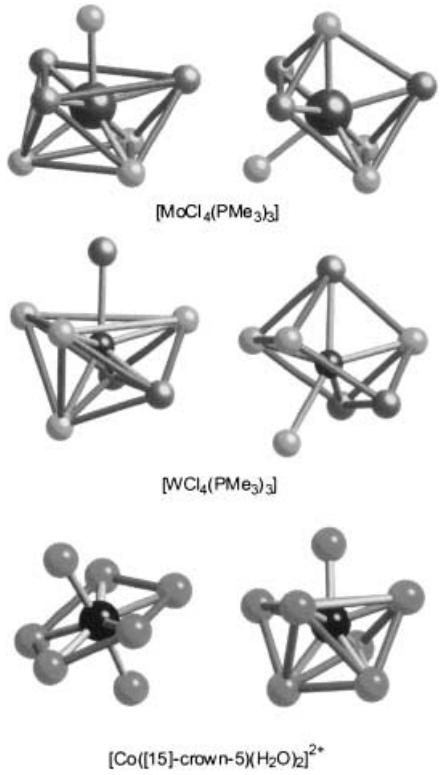

Figure 4. Coordination polyhedra of three sample heptacoordinate complexes in which different polyhedra are superimposed on the same experimental structure to show the similarity of those polyhedra at first sight (see Table 4 and Supporting Information for references and symmetry measures).

Table 2. Proposed[4] geometries and calculated shape measures relative to conventional polyhedra for some examples of heptacoordinate tungsten complexes. The values in boldface indicate the smallest shape measure for a given structure.

Compd.	Proposed polyhedron	PB	CO	CTP	Closest polyhedron	ref.
$[WI_2(CO)_3(CNMe)_2]$	CO	7.09	**2.32**	2.88	CO	icbicw
$[WI_2(CO)_3(NCMe)(SbPh_3)]$	CTP	8.44	**2.51**	3.46	CO	yevfag
$[WI(CO)_3([9]aneS_3)]^+$	4:3	6.63	**1.90**	2.09	CO	tundel
$[WI(acac)(CO)_2(PEt_3)_2]$	PB	4.82	4.44	4.08	none	poyfis

idealized descriptions are or, in other words, how much do the real structures deviate from ideality and in which direction.

A breakdown of the whole set of retrieved structures by central metal has already been presented in the introductory section (Figure 1). The electron configuration of the metal atoms in most complexes of the selected families is seen to present from 0 to 4 electrons in the d manifold, with the d^4 configuration being the most common, in agreement with the expectations of the 18-electron rule. Only those compounds having at least four N- or O-donor atoms and a first-row transition-metal atom, or a Zn group metal, have five or more d electrons.

A broad perspective of the symmetry measures of such a collection of structures can be obtained by plotting them in symmetry maps (Figure 5). Figure 5 shows that there are numerous structures close to the reference CO, CTP, and PBP polyhedra, but also that these are outnumbered by the structures which significantly deviate from the reference shapes. Comparison with Figure 3 clearly indicates that no heptagonal structures were found, and only one point is relatively close to the ideal hexagonal pyramid region (20,20 point in the cCO/cCTP symmetry map); this point, however, corresponds neither to a hexagonal pyramid nor to a trigonal-face-capped trigonal prism. There are only six structural data sets, corresponding to five different compounds (shown as squares in Figure 5) that deviate from the general behavior, best seen in the PBP/cCO map (Figure 5b): 1) One of the Ti atoms in two crystallographically independent molecules in $[Ti_2Me_8]^-$ is described as coordinated by three methyl groups and by three hydrogen atoms of another methyl group that acts as a bridge;[38] this structure is best described as a trigonal bipyramid with the η^3-methyl group occupying an axial coordination position (Figure 6a), although it could also be described as a capped octahedron (Table 3) with the base formed by the three agostic H atoms; the bond angles corresponding to such a trigonal bipyramid are responsible for the large value of S(cCO) in this case. 2) The Fe atom in $[FeH_3(PPh_2nBu)_3(SnMe_3)]$ also presents[39] a CO coordination sphere which, nevertheless, is far from our conventional CO because the three ligands in the capped face are hydrides (see Table 3), most probably the large S(cCO) value is due to differences in bond distances (see angles in Table 3). An alternative description of such a structure would be an FeP_3Sn tetrahedron (actually this core is close to the tetrahedron, with $S(T_d) = 0.85$), with three faces capped by hydrides (Figure 6b). 3) A similar CO is found (Figure 6c) for the W atom in $[WH_3(N\{EtNSiMe_3\}_3)]$,[40, 41] but in this case the hydrides occupy the basal face (Table 3). 4) An approximate 5:2 geometry would describe the unusual coordination geometry of Ag ($S(C_5) = 1.84$ for Ag and the five basal ligands) in a complex with an antibiotic[42] (Figure 6d), and in an

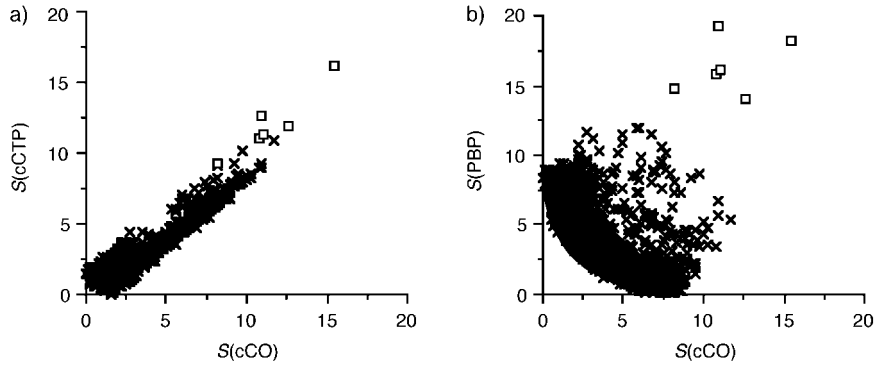

Figure 5. Symmetry maps of the experimental structures of σ-heptacoordinate complexes. The positions of the conventional polyhedra in the symmetry maps can be seen in Figure 3. The outliers (squares) are discussed in the text.

0947-6539/03/0906-1286 $ 20.00+.50/0 *Chem. Eur. J.* **2003**, *9*, No. 6

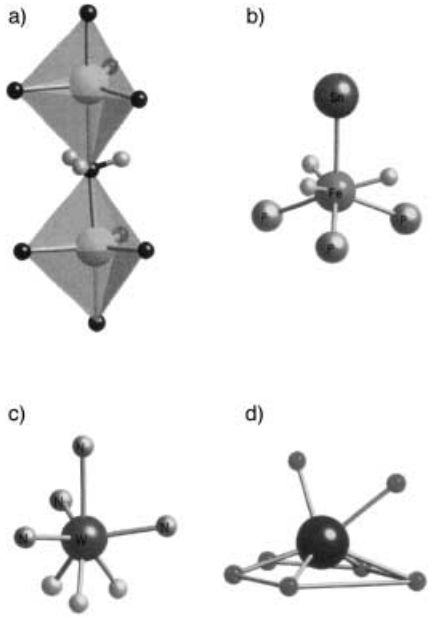

Figure 6. Coordination sphere around the metal atoms in a) $[Ti_2Me_8]^-$ considering the bridging methyl group as monodentate, b) $[FeH_3(PPh_2nBu)_3(SnMe_3)]$, c) $[WH_3(N\{EtNSiMe_3\}_3)]$, d) antibiotic A-130 A-silver(I).

[15]crown-5 ether complex ($S(C_5) = 5.16$)[43] that could alternatively be described as a pentagonal antiprism with a Ag ion sandwiched between two crown ethers, one of which has three oxygen atoms at long distances to Ag.

Let us now go back to the search for the closest conventional polyhedra. We first looked for molecular structures that correspond to a nearly perfect polyhedron, arbitrarily associated with a shape measure smaller than 1.0. Since some cases may present small values for both S(cCO) and S(cCTP), we assign for the present purposes the polyhedron with the smallest shape measure. The first conclusion is that only about one third of the structures can be unambiguously identified with one of the three conventional polyhedra according to such criteria. Still more interesting is the fact that the pentagonal bipyramid is significantly more abundant (20%), whereas the nearly perfect capped octahedron and the capped trigonal prism have similar abundances (7% each).

A different, less restrictive approach consists in searching for the conventional polyhedron that best describes the coordination sphere of each compound, still accepting some degree of distortion from ideality but not severe distortions, represented by shape measures larger than 5.0. In that case, a unique assignment can be applied to most structures, while a few remain unassigned.[44] The assignment of polyhedra for our reference data set is summarized in Table 4, where breakdown by families is also shown. The number of PBP structures (47%) again dominates heptacoordination, but COs (21%) and CTPs (24%) combined have practically the same abundance, leaving 8% of structures that cannot be assigned to any of these polyhedra. It is remarkable that a similar analysis for σ-bonded heptacoordinate rare earth

Table 3. Nonconventional capped octahedral structures (see **8** for the definition of bond angles). The corresponding angles for the conventional CO are also given for comparison.

M	Capping ligand	Capped face	Basal face	α	β	S(cCO)	$S(C_3)$	refcode
Fe	$SnMe_3$	H^-	PPh_2nBu	76	115	10.94	0.00	poswoj
W	N(tripod)	N(tripod)	H^-	78	146	8.21	0.01	zagkey01
Ti	CH_3	CH_3	H	90	160	10.73	0.07	kelqoh
cCO				74.1	125.5	0.00	0.00	

Table 4. Summary of the polyhedral distribution of σ-bonded heptacoordinate transition-metal compounds according to their shape measures.[a]

Family	Subfamily	PBP	CO	CTP	Other	Unassigned	Total
all σ-bonded and metalloproteins		443	195	232	58	20	948
monodentate ligands		16	43	25		5	89
	homoleptic	8	11	15		3	37
	$[Mo(CO)_4X_3]^-$	0	12	2		0	14
	$[M(CO)_3L_nX_{4-n}]$	0	16	3		0	19
	$[M(PR_3)_3X_4]$	0	3	1		2	6
	$[M(thf)_nX_{7-n}]^+$ ($n = 4,5$)	5	0	0		0	5
	$[MXL_6]$	4	1	3		0	8
bidentate ligands		38	19	22		4	83
	$[M(NO_3)_2L_3]$	12	0	0		1	13
	$[M(dtc)_3L]$	15	0	0		0	15
	$[M(carbox)_2L_3]$	10	0	0		0	10
	$[M(diphos)L_5]$	0	14	7		1	22
	$[M(diphos)_2L_3]$	1	5	15		2	23
multidentate ligands		72	8	8		3	91
	[M(**10**)L_2]	23	0	0		0	23
	$[M(O_5\text{-crown})L_2]$	34	0	0		1	35
	$[M(N_5\text{-macrocycle})L_2]$	13	0	0		0	13
	$[M(tacn)L_4]$	1	1	3		0	5
	$[M(tpb)L_4]$	1	7	5		2	15
metallobiomolecules		5	0	3		5	13
dihalobridged [b]		16	6	5		3	30
cyclobutadiene [b]		0	0	0	26 4:3	0	26
alkaline-metal crown-6 [b]		0	0	0	32 HP	0	32

[a] A polyhedron is assigned for the reference shape giving the smallest symmetry measure; structures whose shape measures are all larger than 5.0 are unassigned. [b] Not comprised in the σ-bonded structural data set.

  0947-6539/03/0906-1287 $ 20.00+.50/0

complexes gives a quite similar distribution (46, 27, and 26% of PBP, CO, and CTP structures among 288 structural data sets from 242 independent structural determinations; the corresponding symmetry maps are provided as Supporting Information, Figure S1). While these numbers reflect the overall distribution, we will see below that significant different distributions can be found within a given family. An interesting finding is that in no case the shape measures studied exceed 20 (maximum CSM values found: 15.5, 16.2, and 19.3 for PBP, cCO, and cCTP, respectively). Comparison of those limiting values with Figure 3 tells us that the presence of heptagons among the σ-bonded structures can be excluded. Similarly, hexagonal pyramids, if present at all, must be significantly distorted.

Next, some families of heptacoordinate compounds that were found to present a significant number of members were studied separately. The families analyzed, and the corresponding results, are summarized in Table 4. Data for complexes with monodentate ligands are given in Tables 5 and 6, whereas data for other families are provided as Supporting Information.

Hepta(monodentate) complexes: Data for homoleptic complexes are presented in Table 5, and those for several families of mixed ligand complexes in Table 6. Most of these compounds are seen to have one shape measure of less than 1.0 and an ideal polyhedron can be unequivocally associated to their coordination spheres. For these compounds, all having d^0 to d^4 electron configurations, no clear structural preference exists, according to the dispersion of their shape measures. This finding agrees well with the similar molecular orbital diagrams of the three conventional polyhedra[22] that show two nonbonding and three metal–ligand antibonding d orbitals, thus making heptacoordination unfavorable for electron configurations with five or more d electrons.

If we analyze the results according to the nature of the ligands we find no clear structural preferences among the homoleptic complexes and even the same anion may appear as different polyhedra depending on the counterion, as happens for $[WF_7]^-$, or even two shapes can be found for the two crystallographically independent molecules in the asymmetric unit of $[Mo(CO)_4Br_3]$. Such a structural variability cannot be overemphasized, since there is a tendency to ascribe structural preferences based on a limited amount of data. Hence, we see in Table 5 that $[ZrF_7]^{3-}$ appears mostly as a CTP but an example of a PBP is also known, yet we can find in the literature the assertion that $[ZrF_7]^{3-}$ prefers the PBP structure.[45, 46]

Among the mixed-ligand complexes, those with three or four carbonyl or phosphine ligands present CO (most common) or CTP structures, but not PBP. The most perfect examples of CO-CTP structures seem to correspond to the tetrahalo-tris(phosphine) complexes ($0.19 \le S \le 0.60$), and their deviations from either the CO or CTP polyhedra will be discussed below with respect to the pathway for their interconversion. In contrast, the families of tetrahydrofuran compounds of formulae $[M(thf)_4L_3]$ and $[M(thf)_5L_2]$ prefer the PBP geometry. Although only five such structures have been found, having M = Y or La, the same trend is found among the rare earth analogues (the corresponding symmetry map is provided as Supporting Information, Figure S2). A few complexes with six identical monodentate ligands, $[MXL_6]$ have been identified. Structural variability seems again to be the rule. The only apparent trend is that oxo complexes present the PBP geometry, with the oxo ligand occupying an axial position. However, such a conclusion should be drawn with care since we have only three structural data sets at hand.

Table 5. Shape measures of homoleptic heptacoordinate complexes. The values in boldface indicate the closest polyhedron according to the continuous shape measures.

Compound	Closest polyhedron	d^n	*S*(PBP)	*S*(cCO)	*S*(cCTP)	ref[a]
σ donors						
$[MoMe_7]^-$	CO	0	8.75	**0.42**	1.89	lojdod
$[WMe_7]^-$	CO	0	8.61	**0.36**	1.77	retnej
$[WMe_7]^-$	CO	0	8.67	**0.28**	1.79	retnin
$[RuH_7]^{3-}$	PBP	4	**0.98**	6.34	5.41	$Na_3[RuH_7]$
$[OsH_7]^{3-}$	PBP	4	**0.37**	6.94	5.71	$Na_3[OsH_7]$
π donors						
$[ScF_7]^{4-}$	CTP	0	6.22	2.01	**0.58**	Sr_2ScF_7
$[ZrF_7]^{3-}$	CTP	0	4.99	1.74	**0.36**	dadvin
	CTP	0	4.97	1.66	**0.36**	enfzrb10
	CTP	0	6.22	1.15	**0.35**	enfzrb10
	PBP	0	**0.25**	6.71	5.13	pivvar
	CTP	0	7.04	2.10	**0.77**	$NaBaZrF_7$
$[HfF_7]^{3-}$	PBP	0	**0.24**	7.73	6.16	Ag_3HfF_7
	PBP	0	**0.09**	8.41	6.68	$KPdHfF_7$
$[NbF_7]^{2-}$	CTP	0	6.18	1.19	**0.39**	K_2NbF_7
$[TaF_7]^{2-}$	CTP	0	6.25	1.19	**0.37**	K_2TaF_7
$[MoF_7]^-$	CO	0	5.23	**0.84**	1.13	zobgig
	CO	0	8.26	**0.33**	1.69	$CsMoF_7$
	CO-CTP	0	4.49	**0.95**	**0.89**	zobgus
$[WF_7]^-$	CTP	0	4.02	1.52	**1.25**	yidbes
	CO	0	8.29	**0.36**	1.32	$CsWF_7$
$[ReF_7]$	PBP	0	**1.13**	3.78	3.00	ReF_7
ZrO_7	CO	0	5.82	**1.16**	1.34	monocl.-ZrO_2
		0	11.23	**3.07**	**3.16**	orthorh.-ZrO_2
$[Sc(H_2O)_7]^{3+}$		0	**2.08**	2.76	**2.17**	hosfok
π acceptors						
$[V(CN)_7]^{4-}$	PB	2	**0.14**	7.90	6.19	6083
$[Mo(CN)_7]^{4-}$	CTP	3	2.39	2.69	**1.36**	86685
$[La(NCS)_7]^{4-}$	CTP	0	6.79	1.70	**0.42**	kerhuk
$[Mo(CN)_7]^{4-}$	CTP	3	3.90	1.68	**0.72**	86686
	CTP	3	4.08	1.69	**0.76**	280015
	CTP	3	5.66	4.05	**0.50**	bocmel
$[Ta(CN\text{-}Xyl)_7]^+$	CO	4	6.99	**0.50**	0.66	wodnos
$[Cr(CNBu)_7]^{2+}$	CO	4	4.93	**0.61**	1.17	begsov
$[Mo(CN)_7]^{5-}$	PBP	4	**0.22**	7.99	6.35	200038
$[Mo(CNMe)_7]^{2+}$	CO	4	5.43	**0.50**	0.77	hpmimo
$[Mo(CNPh)_7]^{2+}$	CO	4	6.08	**0.50**	0.75	bezfuh
$[Mo(CNBu)_7]^{2+}$	CTP	4	6.65	1.54	**0.01**	ibicmo
$[W(CNBu)_7]^{2+}$	CTP	4	6.69	1.52	**0.03**	bavxur

[a] Alphabetic characters correspond to the CSD refcodes, numeric entries to ICSD collection codes.

Complexes with bidentate ligands: We have identified five families of complexes with bidentate ligands (**10**) that have a significant number of structures, corresponding to the general formulae $[M(NO_3)_2L_3]$, $[M(carboxylate)_2L_3]$, $[M(dtc)_3L]$, $[M(chel)L_5]$, and $[M(chel)_2L_3]$ (dtc = dithiocarbamate; chel = bidentate ligands forming five-membered chelate rings, such as 1,2-bis(diphenylphosphino)ethane (dppe)). According to the calculated shape measures (data provided as Support-

0947-6539/03/0906-1288 $ 20.00+.50/0 *Chem. Eur. J.* **2003**, *9*, No. 6

Table 6. Shape measures of several families of mixed-monodentate ligand heptacoordinate complexes. The values in boldface indicate the closest polyhedron according to the continuous shape measures.

Compd. M	X/L[a]	Closest polyhedron	d^n	*S*(PBP)	*S*(cCO)	*S*(cCTP)	ref[b]
$[Mo(CO)_4X_3]^-$							
Mo	I	CO	4	9.87	**2.71**	3.63	feykoj
Mo	Br	CTP	4	8.21	1.81	**1.42**	jumcav
		CO		8.57	**1.47**	2.56	
Mo	I	CO	4	9.83	**2.40**	3.49	kabzui
W	Br	CO	4	8.79	**1.42**	2.52	dukcuh
W	I	CO	4	8.32	**2.05**	2.46	lepdit
		CO		8.51	**2.48**	3.35	
W	I	CTP	4	7.99	3.04	**1.79**	lepdoz
				0–98	**2–40**	3.71	
W	Cl	CO	4	8.98	**1.71**	2.79	nuwsaz
W	I	CO	4	10.07	**2.38**	3.67	sarnii
W	Cl	CO	4	7.95	**0.86**	1.80	yocsis
W	Cl	CO	4	8.17	**0.95**	1.98	yocsoy
		CO		7.95	**1.02**	1.98	
$[M(CO)_3L_nX_{4-n}]$							
Nb		CO	4	8.09	**1.92**	2.16	sodzug
Ta		CTP	4	6.04	3.29	**1.67**	cusmim
		CTP		5.68	2.96	**1.75**	
Ta		CO	4	7.79	**1.82**	2.03	cuyzeb
Mo		CO	4	8.38	**1.35**	2.13	tcdcpm
W		CTP	4	8.36	2.69	**2.03**	cipwpb
W		CO	4	9.35	**2.53**	3.71	gifgad
W		CO	4	8.55	**2.59**	3.41	givqad
W		CO	4	9.06	**2.31**	3.29	givqeh
W		CO	4	9.37	**2.75**	3.58	payyet
W		CO	4	9.05	**2.95**	3.75	sabcut
W		CO	4	8.78	**1.93**	2.93	suqmew
W		CO	4	7.66	**2.51**	2.74	tundip
W		CO	4	7.60	**1.87**	2.70	yevduy
W		CO	4	8.44	**2.51**	3.46	yevfag
W		CO	4	9.38	**2.38**	3.34	yundug
W		CO	4	9.50	**2.69**	3.69	yuvtoy
W		CO	4	7.90	**2.62**	3.06	zabnev
W		CO	4	8.68	**2.37**	3.27	zabniz
$[M(PR_3)_3X_4]$							
Nb	Br	CTP	1	5.49	0.92	**0.45**	devyos
Nb	Cl	CO-CTP	1	7.17	**0.60**	**0.60**	gijbuw
Ta	Cl	CO-CTP	1	6.98	**0.58**	**0.58**	cukrij
Mo	Cl	CO	2	8.91	**0.19**	1.81	cmpmoc
Mo	Cl	CO	2	7.89	**0.14**	1.43	mppcmo10
W	Cl	CO	2	7.39	**0.23**	0.80	cugsus
$[M(thf)_nX_{7-n}]^+$ ($n = 4, 5$)							
Y	Cl, O	PBP	0	**0.27**	7.65	5.98	kelsup
Y	Cl	PBP	0	**0.44**	6.30	4.65	pehjan
La	I_2	PBP	0	**1.04**	8.68	6.92	riktag
La	Br_3	PBP	0	**1.23**	6.07	4.87	rigruu
La	I_3	PBP	0	**1.49**	7.89	6.35	ronmem
$[MXL_6]$							
$[NbOF_6]^{3-}$		PBP	0	**0.48**	6.26	4.83	Na_3NbOF_6
$[W(CN)_6O]^{2-}$		PBP	0	**0.38**	7.98	6.31	vecguf10
$[WF_6(CF_3CH_2O)]^-$		CO	0	5.78	**0.64**	1.43	joncaq
$[WF_6(Fpy)]$		CTP	0	6.64	1.89	**0.72**	lahrob
$[ReOF_6]^-$		PBP	0	**0.23**	8.61	6.85	$CsReOF_6$
$[V(CN)_6(NO)]^{4-}$		PBP	4	**0.31**	7.87	6.25	1451
$[Mo(CNBu)_6Br]^+$		CTP	4	6.72	2.51	**0.73**	tbicmo
$[Mo(CNBu)_6I]^+$		CTP	4	7.09	3.14	**1.25**	buicmo

[a] X represents anionic and L neutral ligands. [b] Alphabetic characters correspond to the CSD refcodes, numeric entries to ICSD collection codes.

ing Information) all the compounds in the first three families show a clear preference for the PBP. In the first two families, the bidentate ligands occupy equatorial positions, whereas in the dithiocarbamato complexes one of the ligands occupies one equatorial and one axial position, forcing a deviation of one S donor atom from the ideal axial position. The only exception to the preference for the bipyramid is found among the family of nitrato complexes, in the structure[47] of $[Co(NO_3)_3(NCMe)]^-$ that is isosymmetric (that is, has the same value of the shape measures) with respect to the three conventional polyhedra.

According to the bite angle criterion, one should expect other small bite ligands to favor the PBP geometry; that is actually confirmed by one complex with two bis(diphenylphosphino)methane (dppm) ligands, $[MoI_2(dppm)_2(CO)]$[48] (average bite angle of 72°), for which the *S*(PBP) value is 1.58. Along the same line, we will see below that in difluoro-bridged dinuclear complexes the bond angle imposed by the M_2F_2 core seems to favor the PBP. Conversely, the complexes with a dppe ligand (bite angle of 83°) and the like give a PBP structure only for a La compound[49, 50] but CO, CTP, or intermediate structures in all other cases.

Complexes with multidentate ligands: The symmetry measures of a variety of heptacoordinate complexes with multidentate ligands are provided as Supporting Information and summarized in Table 4. The extended tripod ligand pytren (**11**) and its analogue with exocyclic N–C single bonds have been found to form heptacoordinated complexes with Mn. These two complexes[51, 52] are clearly in the CO geometry, (*S*(cCO) = 0.61 and 0.91, respectively) and further exploration of heptacoordination with this ligand seems worth pursuing.

The quite rigid tridentate macrocyclic ligand triazacyclononane (tacn, **12**) seems to be well adapted to occupy the uncapped face of the CO. The experimental structures of complexes of the type $[M(tacn)L_4]$ (data provided as Supporting Information) are found as CO[53] or CTP[54, 55] structures, and complexes with the analogous sulfur macro-

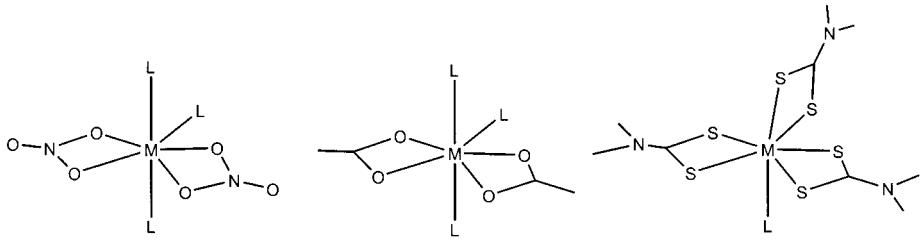

$[M(NO_3)_2L_2]$ $[M(carboxylate)_2L_3]$ $[M(dtc)_3L]$

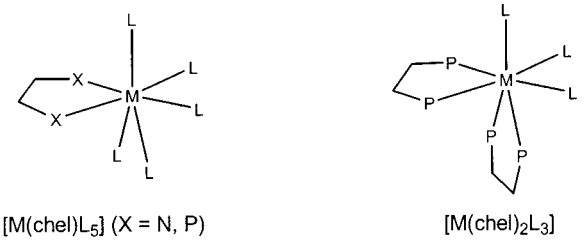

$[M(chel)L_5]$ (X = N, P) $[M(chel)_2L_3]$

10

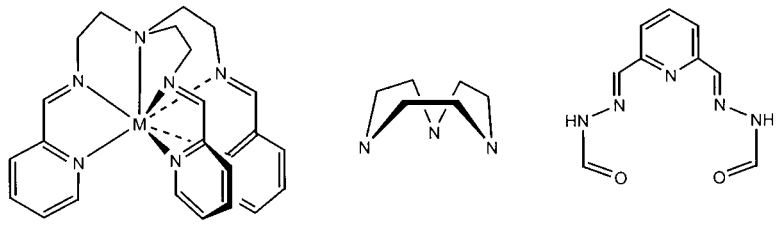

11 **12** **13**

cycle [9]ane-S_3 also present CO coordination spheres.[56, 57] The coordination sphere of one tacn complex[58] seems to be closer to the PBP geometry, but this has a side-bound peroxo ligand. If the peroxo ligand is considered to occupy one coordination position, octahedral coordination might be expected and the approximate PBP shape indicates that it is nearly coplanar with three other *mer* ligands. The tridentate tris(pyrazolyl)borato ligand, even if significantly more flexible than tacn, behaves in a similar way, giving CO and CTP geometries, but not PBP ones.

The complexes with the pentadentate [15]crown-5 ether are practically all PBP (data provided as Supporting Information), with the crown ether occupying the equatorial plane of the bipyramid. The only exception is a Cd complex[59] with a structure that is nearly isosymmetric relative to the three ideal polyhedra. In this structure, the coordination sphere of the Cd^{2+} ion is completed with two bridging bromide ions, a feature that requires a *cis* arrangement of the two bromides. Hence, the macrocycle is folded to occupy four equatorial and one axial position, whereupon two of the equatorial O donors are strongly pulled away from the mean equatorial plane. A few complexes with other pentadentate macrocyclic compounds all form pentagonal bipyramids with the macrocyclic ligand in the equatorial planes, but even a semirigid open-chain pentadentate ligand such as the one shown in **13** yields PBP geometries with first row transition metals in a variety of electron configurations.

Dihalo-bridged dinuclear complexes: A significant number of heptacoordinate compounds appear as di- or polynuclear units. So far we have disregarded di- and polynuclear complexes from our analysis, in order to restrict any conclusions about stereochemical preferences to the interplay of metal–ligand bonding and ligand–ligand repulsions, without the constraints imposed by bridging ligands. Now we loosen the restriction to see if we can obtain some relevant information on the effect of bridging ligands. To that end, we have analyzed the family of di- and polynuclear complexes bridged by two halides (data supplied as Supporting Information) and the results are summarized in Table 4.

Most Zr and Hf complexes with fluoro bridges present rather small F-M-F bridging angles ($65.1 \pm 0.3^\circ$ for ten structural data sets of eight compounds) and appear as nearly perfect pentagonal bipyramids, as expected from the bite angle criterion discussed above. The exceptions are compounds with two small-bite bidentate ligands[60] and polynuclear compounds,[61–63] for which the PBP is no longer the best option, as well as a Cd compound coordinated by a pentadentate crown ether in addition to the two halo bridges. Another PBP corresponds to a bromo-bridged complex with a bite angle of 90°. While the fluoro bridges occupy two equatorial positions (ideal bite angle of 72°), the bromo bridges occupy one equatorial and one axial position (ideal bite angle of 90°) of the PBP.

4:3 Coordination geometry: The 4:3 geometry (**6**) has been proposed for the coordination spheres of the metal atoms in the monoclinic form of ZrO_2,[51] as well as for the cationic complex[4] $[WI(CO)_3([9]aneS_3)]^+$. The corresponding shape measures tell us that the former (Table 4) is better identified as a CO as a good approximation. For $[WI(CO)_3([9]aneS_3)]^+$, the shape measures (Table 2) tell us that the W coordination polyhedron is in between the cCO and the cCTP as for many homoleptic complexes discussed above. Does such a small distortion from the ideal cCO and cCTP warrant a description as a distinct 4:3 polyhedron? To answer this question, we have to analyze the symmetry measures of compounds that can be clearly described as sandwiches of a metal atom between a triangle and a square, namely the cyclobutadiene complexes of general formula $[M(\eta^4\text{-}C_4R_4)L_3]$. All these complexes (data provided as Supporting Information) consistently appear in a region of the cCO/cCTP symmetry map that is far away from the conventional polyhedra, with CSM values larger than 13.76, 9.05, and 8.23 relative to PBP, cCO, and cCTP,

0947-6539/03/0906-1290 $ 20.00+.50/0 *Chem. Eur. J.* **2003**, *9*, No. 6

respectively. These structures appear forming two clusters of points in the symmetry map (Figure 7) that correspond to the subfamilies with L = CO and L = Cl.

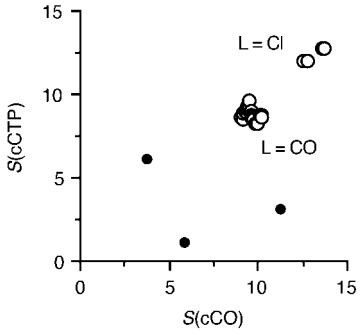

Figure 7. Position of the $[M(\eta^4\text{-}C_4R_4)L_3]$ complexes in the cCO-cCTP symmetry map (open circles). The monoclinic form of ZrO_2 and $[WI(CO)_3([9]aneS_3)]^+$, which have been previously assigned a 4:3 geometry, are also shown for comparison (closed circles).

Returning to $[WI(CO)_3([9]aneS_3)]^+$, its symmetry measures appear in a quite different region of the cCO/cCTP symmetry map than the cyclobutadiene complexes (Figure 7) and it was probably assigned the 4:3 geometry because the tridentate nature of the macrocyclic ligand visually suggests such a simplified description. A closer look at the structural data shows that the basal face of the 4:3 polyhedron formed by the four monodentate ligands is strongly distorted from a square (for example, the C-I-C angle is 62.5° and $S(C_4)$ for the four monodentate ligands is 3.98). Similarly, the ZrO_7 group in the monoclinic form of ZrO_2 falls well off the 4:3 region of the symmetry map.

Hexagonal pyramids: Among the structures disregarded for having disorder or high *R* values we were surprised to find a silver compound[64] far away from the three conventional polyhedra: $S(PBP) = 23.23$, $S(cCO) = 18.19$ and $S(cCTP) = 20.62$ for one of the two crystallographically independent molecules, and similar values for the other one. The coordination sphere of the silver ion in such a compound turned out to be a hexagonal pyramid, characterized by $S(C_6)$ values of 1.43 and 1.10 for the two crystallographically independent silver ions and *S*(HP) values of 1.57 and 1.22. We have been unable to identify such a geometry in any other transition metal complex. To facilitate the future identification of new hexagonal pyramidal structures of transition metals we tried to pinpoint a variety of structurally characterized hexagonal pyramids, and these were found among the [18]crown-6 complexes of alkaline metals. Among these, those that have approximately a sixfold symmetry axis (that is, $S(C_6) < 3.6$) are presented in the symmetry maps (Figure 8, data provided as Supporting Information). Comparing those structures with our reference hexagonal pyramid, we found a fair correlation between shape -*S*(HP)- and symmetry -$S(C_6)$- measures: $S(HP) = 0.05 + 1.41\ S(C_6)$ ($r^2 = 0.892$ for 33 data sets). In contrast, no correlation is found between $S(C_6)$ and the other shape measures (PBP, cCO, and cCTP).

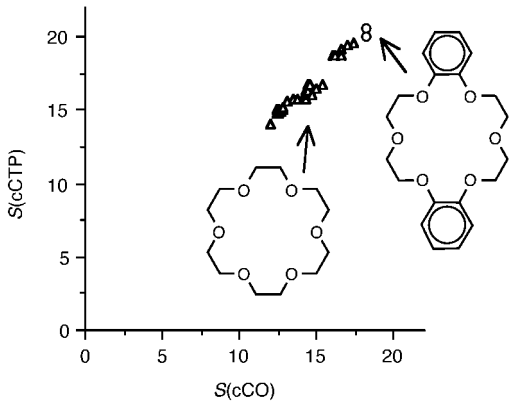

Figure 8. Position in the cCO – cCTP symmetry map of the heptacoordinate [18]crown-6 complexes of alkaline-metal ions (triangles, data provided as Supporting Information), and of a related Ag complex (circles, see text for reference).

Interestingly, the structures of the alkaline metal complexes in Figure 8 form two clusters of points. The group of structures with larger shape measures are seen to correspond to compounds with two benzo rings in the crown ether and all of them appear close to the ideal hexagonal pyramid (*S*(HP) values of less than 1.3). Complexes with unsubstituted ligands, on the other hand, are slightly closer to the cCO and cCTP but their hexagonal pyramidal measures are more variable (between 0.5 and 6.3). One compound with only one benzo group has also been found, which appears in the symmetry map among the unsubstituted ligands.

Metallobiomolecules: The metallobiomolecules with heptacoordinate metal centers retrieved from the MDB are shown in Table 7, together with their symmetry measures. None of

Table 7. Shape measures for the coordination sphere of heptacoordinate transition-metal centers in metallobiomolecules. The values in boldface indicate the closest polyhedron according to the continuous shape measures.

M	PBP	cCO	cCTP	Compound/source	PDB code
Mo	7.46	8.90	8.14	dmso reductase/*Rhodobacter capsulatus*	1dmr
Mo	5.74	5.54	4.62	oxidized dmso reductase/*Rhodobacter capsulatus*	1e5v
Mn	**3.68**	6.97	6.27	arginase (hydrolase)/*Rattus norvegicus*	1d3v
Mn	5.74	3.52	**2.18**	manganese concanavalin A/*Canavalia ensiformis*	1dq5
Mn	5.38	3.52	**1.81**	sugar-binding protein/*Canavalia ensiformis*	dq6
Mn	4.42	3.25	**2.58**	glutamine synthetase/*Salmonella typhimurium*	1f52
Mn	5.49	9.11	8.38	L-fucose isomerase/*Escherichia coli*	1fui
Mn	5.58	7.14	6.54	hydrolase/*Methanococcus jannaschii*	1g0i
Mn	**3.10**	4.64	3.87	Mn complex troponin-C/*Gallus gallus*	1ncy
Cd	**1.80**	8.93	7.38	oxidoreductase/*Phanerochaete chrysosporium*	1d7b
Cd	**0.66**	5.93	4.42	carrageenase complex/*Pseudoalteromonas carrageenovora*	1dyp
Cd	6.56	4.78	4.58	alkaline cellulase/*Bacillus sp.*	1g0c
Cd	**3.59**	4.88	4.06	troponin C (Ca binding-protein)/*Gallus gallus*	1ncx

the structures given in the table are close to the cCO or cCTP shapes, while some of them are quite close to the PBP. In fact, all those structures are nicely placed along the pathway from CO and CTP to the PBP (see discussion below and Figures 9 and 12).

Interconversion pathways: The maximum symmetry pathways for the interconversion of the PBP, the CO, and the CTP[22, 23] correspond to the symmetry group C_s, a common subgroup of each pair of ideal symmetries (D_{5h}, C_{3v}, and C_{2v}). Thus only a symmetry plane can be preserved along such interconversion pathways, which corresponds in the schematic representation **14** to the plane formed by ligands c, d, and e.

These pathways therefore offer good study cases to be analyzed in terms of continuous symmetry measures. As an example, when going from the CO to the CTP we should be able to see how the C_3 rotation gradually disappears, the C_2 rotation becomes closer to being a symmetry operation, and the reflection plane σ_v (the cde plane) is preserved. In an analogous way, conversion of the CO (or the CTP) into a PBP must be accompanied by the gradual lose of the C_3 (or C_2) rotation and the gradual appearance of C_5, while σ_v should be retained throughout.

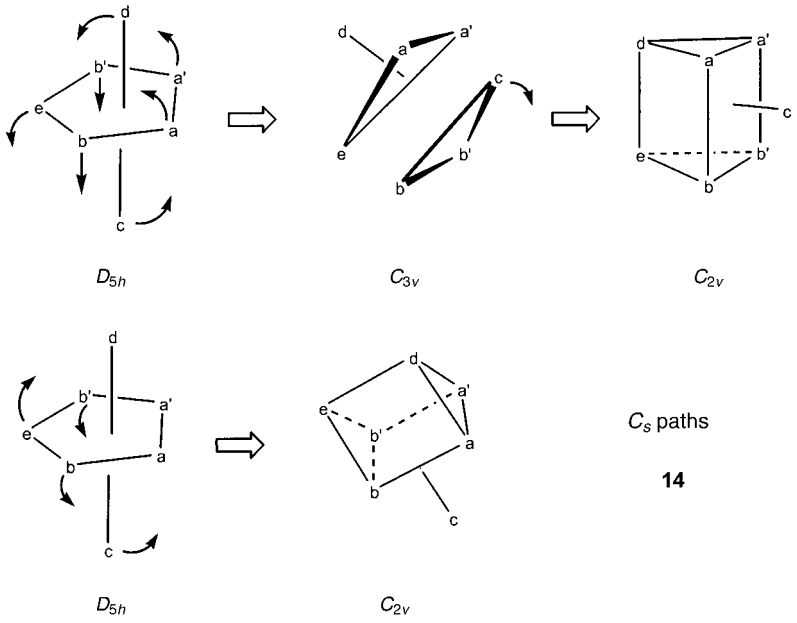

14

Since the symmetry measures have the meaning of the square of a distance to ideal polyhedra, we define the maximum-symmetry pathway between two polyhedra A and B as that which makes the *distance* function δ_{AB} minimum [Eq. (2)]. We have seen in previous work on hexa- and tetracoordinate compounds[31, 33] that such an expression describes to a very good approximation the symmetry measures along polytopal rearrangement pathways if k_{AB} is chosen as the δ_{AB} value obtained from the shape measure of A relative to B (or vice versa), a parameter that we have termed the *symmetry constant* of the A–B interconversion pathway. The symmetry constants for the interconversion of the seven-vertex polyhedra are given in Table 8.

$$\delta_{AB} = \sqrt{S(A)} + \sqrt{S(B)} \leq k_{AB} \quad (2)$$

Table 8. Symmetry constants for the interconversion of seven-vertex polyhedra (**1**–**6**).

	PBP	cCO	cCTP	HP	HEP
PBP	0.000	2.899	2.577	5.166	5.934
cCO		0.000	1.236	4.130	6.146
cCTP			0.000	4.467	5.989
HP				0.000	5.047

If we construct a triangle the edges of which have lengths given by the symmetry constants for the interconversion involving the PBP, CO, and CTP (see **15**), these edges represent the maximum symmetry paths defined by Equation (2). Simple geometry allows us to analytically define the corresponding shape measures as a function of the corresponding distance δ_{AB} (that is, the distance of a given point along the pathway to one of the vertices), and to plot those pathways in a symmetry map (Figure 9, solid lines). An interesting result is that direct interconversion between each pair of polyhedra seems feasible through maximum-symmetry paths. Another interesting finding is that the transformation of a cCO to a PBP is nearly coincident with the path to a cCTP at early stages but then diverges, a result that is imposed by the symmetry constants that determine the triangle in **15**, since the minimum distance to the CTP vertex is at the point indicated by an arrow. Given the large

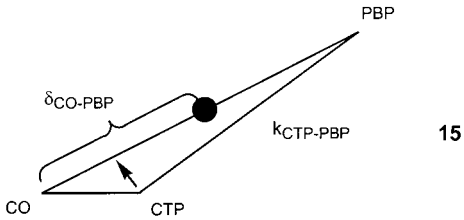

15

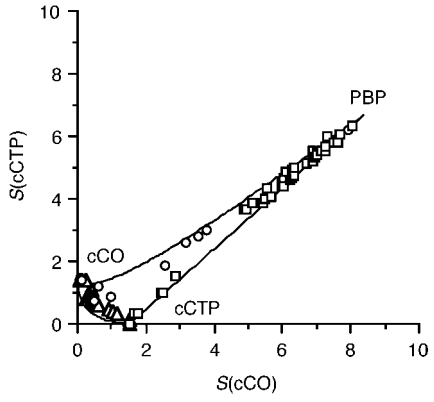

Figure 9. Variation of S(cCTP) as a function of S(cCO) for structures that fall along the CO–PBP interconversion pathway

0947-6539/03/0906-1292 $ 20.00+.50/0 *Chem. Eur. J.* **2003**, *9*, No. 6

separation between the PBP and cCO or cCTP and the close proximity of these two, the two pathways that start at the PBP are practically indistinguishable in the initial stages (for S(cCO) larger than about 6.0). In contrast, the cCTP-CO and cCTP-PBP paths diverge practically from the beginning. It is instructive to compare this symmetry map for the maximum symmetry transformations with the experimental data presented in Figure 5. The behavior of the large amount of structural data is captured in its essence by these geometrical paths, although the variety of structural situations present in the experimental sample results in a widening of the irregular wedge of Figure 9.

We recall that many of the structures (Table 4) could not be unequivocally assigned to a particular polyhedron. It is thus appropriate at this point to ask whether this means that these correspond to geometries that fall along one of the possible interconversion pathways. Looking first at the homoleptic complexes studied here (Table 5) we find that more than half of them appear approximately aligned along the CO–CTP, CO–PBP, or CTP–PBP pathways, characterized by δ_{AB} values of less than 1.70, 3.20, and 2.90, respectively (that is, close to the corresponding symmetry constants of 1.24, 2.90, and 2.60). Among the mixed-ligand complexes (Table 6), the tetrahalotriphosphine family is spread mostly along the pathway for the interconversion between the CO and the CTP ($\delta_{\text{CO-CTP}}$ values between 1.37–1.78, compared to the corresponding symmetry constant, $k_{\text{CO–CTP}} = 1.24$).

In Figure 10 we show several symmetry measures of those structures that fall along the CO–CTP interconversion pathway ($\delta_{\text{CO–CTP}} < 1.7$). Some interesting trends can be observed: a) The structures with S(cCO) values of less than 0.4 have nearly perfect C_3 symmetry, as indicated by $S(C_3)$ values smaller than 0.1; b) the amount of C_3 symmetry and the proximity to the conventional CO show an approximately linear correlation; c) there is a gradual loss of C_3 symmetry as one moves from the CO to the CTP, and d) the C_2 symmetry increases ($S(C_2)$ decreases) along the path from CO to CTP, becoming fully C_2-symmetric for the perfect cCTP (linear correlation with S(cCTP)). Finally, it must be noted that all the structures selected with the $\delta_{\text{CO–CTP}}$ criterion retain a symmetry plane, as indicated by reflection measures smaller than 0.18. Our observation in a previous section, when we defined the conventional CO, that the choice of the reference polyhedron induces an uncertainty in the value of S(cCO) of around 0.2 units is confirmed by the fact that the smallest S(cCO) values are 0.1 to 0.2 units larger than the corresponding $S(C_3)$ value (Figure 10).

As done above for the CO–CTP pathway, we empirically define the shortest pathway between the CO and PBP structures by the corresponding symmetry constant (Table 8) and show in Figure 9 the data for complexes with $\delta_{\text{CO–PB}}$ values of less than 3.20. Again, we can find good correlations between the symmetry measures associated with the C_{3v} and C_{5v} point groups of the two extremes of the interconversion pathway. As examples, the correlations between S(PBP), $S(C_3)$, and $S(C_5)$ are illustrated in Figure 11. As in the above case, a symmetry plane is preserved along the CO–PBP path, as shown by reflection measures of less than 0.31. A similar analysis can be done for the cCTP–PBP pathway.

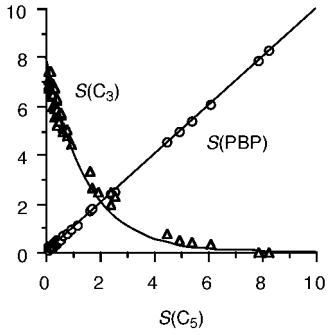

Figure 11. Dependence on $S(C_5)$ of S(PBP) (triangles) and $S(C_3)$ (circles) for complexes that fall along the CO–PBP interconversion pathway, selected according to the criterion $\delta_{\text{CO-PBP}} < 3.20$.

The shape measures of the structures selected with the above criteria nicely reproduce the geometrical lines corresponding to the three maximum symmetry pathways in the cCO–cCTP symmetry map (Figure 9). The maximum-symmetry paths in the above symmetry map can be thus applied to describe in a visual, systematic way the structures of heptacoordinate metal centers in metallobiomolecules discussed above (Figure 12). In such a figure it is clear that the analyzed structures are pentagonal bipyramids with varying degrees of distortion towards the CO and CTP region of the map.

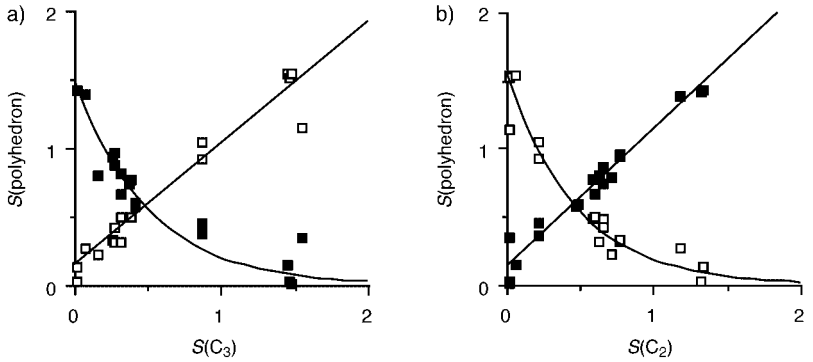

Figure 10. Evolution of the cCO (squares), and cCTP (circles) shape measures as a function of the rotational symmetry measures a) $S(C_2)$ and b) $S(C_3)$ for a set of structures that represent the maximum symmetry interconversion pathway between cCO and cCTP geometries ($\delta_{\text{CO-CTP}} < 1.70$).

Conclusion

For the particular case of heptacoordination, we have chosen conventional reference polyhedra relative to which we obtain the continuous shape measures of the metal coordination spheres. The polyhedra that have been explored include the pentagonal bipyramid (PBP), the capped octahedron (CO), the capped trigonal prism (CTP), the hexagonal

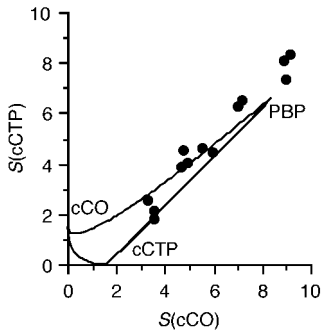

Figure 12. Position of the structures of heptacoordinated metal centers in metallobiomolecules (closed circles) in a cCTP – cCO symmetry map. The positions of the reference polyhedra are also indicated and the maximum-symmetry paths for the interconversion of the three polyhedra are represented by continuous lines.

pyramid (HP), and the heptagon (HEP). The separation between two reference polyhedra depends mostly on differences in their three-dimensional character. Two symmetry maps have been analyzed in which either S(cCTP) or S(PBP) are plotted as a function of S(cCO).

The distribution of heptacoordination throughout the periodic table has been analyzed according to the structural data available in the Cambridge Structural Database. Most heptacoordinate compounds are seen to correspond to metal atoms with d^0 to d^4 electron configurations, the only exceptions being the complexes with N- or O-donor atoms of the first-row transition metals or of the Zn group.

The shape measures S(PBP), S(cCO), and S(cCTP) have been obtained from the experimental structural data of about 1000 heptacoordinate transition metal compounds. Only one third of the analyzed structures can be accurately described by one of the reference polyhedra, with the pentagonal bipyramid being the most common case. For most molecular structures, however an unambiguous assignment of the closest coordination polyhedron can be made by comparing its symmetry measures relative to the three conventional polyhedra and choosing the shape that gives the smallest value. In other cases, the coordination sphere is best described as lying along one of the possible interconversion pathways. No heptagonal and only one hexagonal pyramidal structures were found among transition metals, but it has been shown that hexagonal pyramids present in alkaline-metal complexes can be easily identified through their S(cCO) and S(cCTP) measures. The 4:3 geometry is well differentiated from the conventional polyhedra (PBP, cCO, and cCTP) in the family of cyclobutadiene complexes of formula $[M(\eta^4\text{-}C_4R_4)L_3]$. Other compounds for which a 4:3 geometry has been proposed are best described in terms of one of the conventional polyhedra.

From the analysis of the structures by families, the following conclusions can be drawn:

1) No clear structural preference is found for homoleptic complexes according to their electron configuration or type of ligands.
2) Among mixed monodentate ligand complexes structural preferences are found for some specific families: a) the tetrahalotris(phosphine) complexes $[M(PR_3)_3X_4]$ can be found as CO, CTP, or intermediate structures, but not as pentagonal bipyramids; b) the tetrahydrofuran compounds $[M(thf)_5L_2]$ (M = Y, La) seem to prefer the PBP, and c) oxo complexes of composition $[MOL_6]$ prefer the PBP with the oxo ligand in an axial position.
3) The presence of one or two bidentate ligands with small bite angles (dithiocarbamates, carboxylates, nitrate) favors the PBP structure, with the bidentate ligands occupying the equatorial positions. Exceptions corresponding to polynuclear complexes have been discussed.
4) Among the multidentate ligands analyzed, the extended tripod pytren seems to favor the CO geometry, whereas tridentate ligands such as triazacyclononane and tris(pyrazolyl)borate show a diversity of coordination polyhedra. The pentadentate crown ethers such as [15]crown-5 clearly favor the PBP geometry. The [18]crown-6 and related crown ethers, on the other hand, favor the hexagonal pyramid for the alkaline-metal ions as well as for the only transition-metal complex found with such a type of ligand.
5) Heptacoordinate Mn, Cd, and Mo sites in metallobiomolecules are aligned along the paths that connect the PBP with the CO or the CTP. A few structures are close to PBP but none is close to the other two conventional polyhedra.

The symmetry constant k_{AB} for a polytopal rearrangement between polyhedra A and B has been defined. The maximum symmetry pathway for such a polytopal pathway can be approximated by one along which the sum of the square roots of the corresponding symmetry measures, S(A) and S(B), presents a minimum deviation from the symmetry constant. The analysis of the molecular structures that meet this criterion for the CO – CTP, CO – PBP, and CTP – PBP pathways shows gradual changes in the rotational symmetry corresponding to the C_{5v}, C_{3v}, and C_{2v} point groups of the three polyhedra.

Appendix

A detailed description of the algorithms used to calculate continuous symmetry (or shape) measures defined according to Equation (1) can be found in reference [65] and will only briefly be outlined here. The basic steps to obtain the coordinates P_k of the ideal polyhedron that is closest to an arbitrary distorted polyhedron with vertices at positions Q_k are:

1) The distorted polyhedron is translated so that its center of mass is placed at the origin of coordinates ($Q_0 = 0$). Its orientation, size and vertex labeling are either arbitrary or selected for convenience of computation.
2) The target shape, a size-normalized reference polyhedron, is also placed with its center of mass at Q_0. Its orientation and vertex labeling are also arbitrary.
3) The transformation that the set P_{0k} of vertices of this reference polyhedron has to undergo to yield the desired set P_k that is closest to the distorted polyhedron Q_k is simply $P_k = A\mathbf{R}P_{0k} + \mathbf{T}$, where A is an isotropic scaling factor, $\mathbf{R}$ is a (3×3) rotation matrix, and $\mathbf{T}$ a (3×1) displacement vector.

0947-6539/03/0906-1294 $ 20.00+.50/0 *Chem. Eur. J.* **2003**, *9*, No. 6

4) Minimization to find the ideal polyhedron P_k that is closest (in the root-mean-square sense) to the distorted polyhedron Q_k involves three consecutive minimization steps (minimization with respect to **T**, **R**, and A).
5) Step 4 must be repeated over all possible corresponding pairs between the vertices of the reference and the distorted polyhedron in order to find the vertex labeling that minimizes the distance between the two polyhedra.

Shape and symmetry measures were calculated with the computer programs *sym_he*, *symm*, and *cn*, developed at the Hebrew University of Jerusalem by D. Avnir and M. Pinsky, and *shape*, developed during the present work at the University of Barcelona. Interface programs for transferring a large quantity of data from structural databases to the symmetry measure programs were developed by our group.

Acknowledgements

This work has been supported by the Dirección General de Investigación (DGI), project BQU2002-04033-C02-01. Additional support from Comissió Interdepartamental de Ciència i Tecnologia (CIRIT) through grant 2001SGR-0044 is also acknowledged. The authors thank D. Avnir and M. Pinsky for permission to use their symmetry measure programs *symm* and *cn*.

[1] O. Kahn, J. Larionova, L. Ouahab, *Chem. Commun.* **1999**, 945.
[2] V. Pfennig, N. Robertson, K. Seppelt, *Angew. Chem.* **1997**, *109*, 1410; *Angew. Chem. Int. Ed. Engl.* **1997**, *36*, 1350.
[3] T. Vogt, A. N. Fitch, J. K. Cockroft, *Science* **1994**, *263*, 1265.
[4] P. K. Baker, *Chem. Soc. Rev.* **1998**, *27*, 125.
[5] J. R. Atwood, *Inorganic and Organometallic Reaction Mechanisms*, Wiley-VCH, New York, **1997**.
[6] R. C. Bray, B. Adams, A. T. Smith, B. Benett, S. Bailey, *Biochemistry* **2000**, *39*, 11258.
[7] A. S. McAlpine, A. G. McEwan, A. L. Shaw, S. Bailey, *J. Biol. Inorg. Chem.* **1997**, *2*, 590.
[8] H. S. Gill, D. Eisenberg, *Biochemistry* **2001**, *40*, 1903.
[9] K. A. Johnson, L. Chen, H. Yang, M. F. Roberts, B. Stec, *Biochemistry* **2001**, *50*, 618.
[10] S. T. Rao, K. A. Satyshur, M. L. Greaser, M. Sundaralingam, *Acta Crystallogr. Sect. D* **1996**, *52*, 916.
[11] J. E. Seemann, G. E. Schuz, *J. Mol. Biol.* **1997**, *273*, 256.
[12] B. M. Hallberg, T. Bergfors, K. Backbro, G. Pettersson, G. Henriksson, C. Divne, *Structure (London)* **2000**, *8*, 78.
[13] G. Michel, L. Chantalat, E. Duee, T. Barbeyron, B. Henrissat, B. Kloareg, O. Dideberg, *Structure (Cambridge)* **2001**, *9*, 513.
[14] T. Shirai, H. Ishida, Y. Noda, T. Yamane, K. Ozaki, Y. Hakamada, S. Ito, *J. Mol. Biol.* **2001**, *310*, 1079.
[15] M. G. B. Drew, *Progr. Inorg. Chem.* **1977**, *23*, 67.
[16] D. L. Kepert, *Progr. Inorg. Chem.* **1979**, *25*, 41.
[17] M. Melnik, P. Sharrock, *Coord. Chem. Rev.* **1985**, *65*, 49.
[18] B. W. Clare, D. L. Kepert, in *Encyclopedia of Inorganic Chemistry, Vol. 2* (Ed.: R. B. King), Wiley, New York, **1994**, p. 800.
[19] K. Nakamoto, *Infrared and Raman Spectra of Inorganic and Coordination Compounds. Part B: Applications in Coordination, Organometallic and Bioinorganic Chemistry*, J. Wiley, New York, **1997**.
[20] S. Giese, K. Seppelt, *Angew. Chem.* **1994**, *106*, 473; *Angew. Chem. Int. Ed. Engl.* **1994**, *33*, 461.
[21] H.-B. Bürgi, *Inorg. Chem.* **1973**, *12*, 2321.
[22] R. Hoffmann, B. F. Beier, E. L. Muetterties, A. R. Rossi, *Inorg. Chem.* **1977**, *16*, 511.
[23] E. L. Muetterties, L. J. Guggenberger, *J. Am. Chem. Soc.* **1974**, *96*, 1748.
[24] D. L. Kepert, *Inorganic Stereochemistry*, Springer, Berlin, **1982**.
[25] Z. Lin, I. Bytheway, *Inorg. Chem.* **1996**, *35*, 594.
[26] H. Zabrodsky, S. Peleg, D. Avnir, *J. Am. Chem. Soc.* **1992**, *114*, 7843.
[27] H. Zabrodsky, S. Peleg, D. Avnir, *J. Am. Chem. Soc.* **1993**, *115*, 8278 (Erratum: **1994**, *116*, 656).
[28] F. Maseras, O. Eisenstein, *New J. Chem.* **1997**, *21*, 961.
[29] J. A. K. Howard, R. C. B. Copley, J.-W. Yao, F. H. Allen, *Chem. Commun.* **2000**, 2175.
[30] J. W. Yao, R. C. B. Copley, J. K. H. Howard, F. H. Allen, W. D. S. Motherwell, *Acta Crystallogr. Sect. B* **2001**, *57*, 251.
[31] J. Cirera, P. Alemany, S. Alvarez, unpublished results.
[32] S. Alvarez, M. Llunell, *J. Chem. Soc. Dalton Trans.* **2000**, 3228.
[33] S. Alvarez, D. Avnir, M. Llunell, M. Pinsky, *New J. Chem.* **2002**, *26*, 996.
[34] F. H. Allen, O. Kennard, *Chem. Des. Autom. News* **1993**, *8*, 31.
[35] J. M. Castagnetto, S. W. Hennessy, V. A. Roberts, E. D. Getzoff, J. A. Tainer, M. E. Pique, *Nucleic Acid Res.* **2002**, *30*, 379.
[36] H. B. Thompson, L. S. Bartell, *Inorg. Chem.* **1968**, *7*, 488.
[37] M. G. B. Drew, A. P. Wolters, *J. Chem. Soc. Chem. Commun.* **1972**, 457.
[38] S. Kleinhenz, K. Seppelt, *Chem. Eur. J.* **1999**, *5*, 3573.
[39] S. Gilbert, M. Knorr, S. Mock, U. Schubert, *J. Organomet. Chem.* **1994**, *480*, 241.
[40] D. A. Dobbs, R. R. Schrock, W. M. Davis, *Inorg. Chim. Acta* **1997**, *263*, 171.
[41] R. R. Schrock, K.-Y. Shih, D. A. Dobbs, W. M. Davis, *J. Am. Chem. Soc.* **1995**, *117*, 6609.
[42] H. Koyama, K. Utsumi-Oda, *J. Chem. Soc. Perkin Trans. 2* **1977**, 1531.
[43] P. D. Prince, J. W. Steed, *Supramol. Chem.* **1998**, *10*, 155.
[44] Note: For the compounds with monodentate ligands to be discussed below we have alternatively applied the least-squares criterion of Maseras and Eisenstein and found the resulting assignment of polyhedra to be fully consistent.
[45] B. Douglas, D. H. McDaniel, J. J. Alexander, *Concepts and Models of Inorganic Chemistry*, 2nd ed. J. Wiley, New York, **1983**.
[46] M. Kaupp, *Angew. Chem.* **2001**, *113*, 3642; *Angew. Chem. Int. Ed.* **2001**, *40*, 3535.
[47] J. O. Albright, J. C. Clardy, J. G. Verkade, *Inorg. Chem.* **1977**, *16*, 1977.
[48] F. A. Cotton, R. Poli, *Inorg. Chem.* **1986**, *25*, 3703.
[49] D. R. Cary, J. Arnold, *J. Am. Chem. Soc.* **1993**, *115*, 2520.
[50] D. R. Cary, G. E. Ball, J. Arnold, *J. Am. Chem. Soc.* **1995**, *117*, 3492.
[51] A. Deroche, I. Morgensten-Badarau, M. Cesario, J. Ghilhem, B. Keita, L. Nadjo, C. Houee-Levin, *J. Am. Chem. Soc.* **1996**, *118*, 4567.
[52] M. Qian, S.-H. Gou, L. He, Y.-M. Zhou, C.-Y. Duan, *Acta Crystallogr. Sect. C* **1999**, *55*, 742.
[53] J. E. Ellis, A. J. DiMaio, A. L. Rheingold, B. S. Haggerty, *J. Am. Chem. Soc.* **1992**, *114*, 10676.
[54] P. Chaudhuri, K. Wieghardt, Y.-H. Tsai, C. Kruger, *Inorg. Chem.* **1984**, *23*, 427.
[55] T. Weyhermuller, K. Wieghardt, P. Chaudhuri, *J. Chem. Soc. Dalton Trans.* **1998**, 3805.
[56] P. K. Baker, S. J. Coles, M. C. Durrant, S. D. Harris, D. L. Hubhes, M. B. Hursthouse, R. L. Richards, *J. Chem. Soc. Dalton Trans.* **1996**, 4003.
[57] R. Hart, W. Levason, B. Patel, G. Reid, *J. Chem. Soc. Dalton Trans.* **2002**, 3153.
[58] P. Jeske, G. Haselhorst, T. Weyhermuller, K. Wieghardt, B. Nuber, *Inorg. Chem.* **1994**, *33*, 2462.
[59] R. D. Rogers, A. H. Bond, *Inorg. Chim. Acta* **1996**, *250*, 105.
[60] M. Polamo, M. Leskela, *J. Chem. Soc. Dalton Trans.* **1996**, 4345.
[61] V. V. Tkachev, R. L. Davidovich, L. O. Atovmyan, *Koord. Khim.* **1993**, *19*, 292.
[62] B. C. U. Nair, J. E. Sheats, R. Ponteciello, D. Van Engen, V. Petrouleas, G. C. Dismukes, *Inorg. Chem.* **1989**, *28*, 1582.
[63] A. V. Gerasimenko, I. P. Kondryatuk, R. L. Davidovich, M. A. Medkov, B. V. Bukvetskii, *Koord. Khim.* **1986**, *12*, 710.
[64] L. Zuocai, S. Meicheng, *Beijing Dax. Xue. Zir. Kex. (Acta Sci. Nat. Univ. Pek.)* **1987**, 17.
[65] M. Pinsky, D. Avnir, *Inorg. Chem.* **1998**, 37, 5575.

Received: September 25, 2002 [F4448]